PHOTOSYNTHETICA
International Journal for Photosynthesis Research

DOI 10.32615/ps.2022.019 PHOTOSYNTHETICA 60 (2): 271-279, 2022

Upregulation of the mitochondrial alternative oxidase pathway improves PSII function and photosynthetic electron transport in tomato seedlings under chilling stress

J.J. ZENG, W.H. HU+, X.H. HU, H.M. TAO, L. ZHONG, and L.L. LIU

School of Life Sciences, Jinggangshan University, 343009 Ji'an, China

Abstract

The aim of this study was to explore how the mitochondrial alternative oxidase (AOX) pathway alleviates photoinhibition in chilled tomato (*Solanum lycopersicum*) seedlings. Chilling induced photoinhibition in tomato seedlings despite the increases in thermal energy dissipation and cyclic electron flow around PSI (CEF-PSI). Chilling inhibited the function of PSII and blocked electron transport at the PSII acceptor side, however, it did not affect the oxygen-evolving complex on the donor side of PSII. Upregulation of the AOX pathway protects against photoinhibition by improving PSII function and photosynthetic electron transport in tomato seedlings under chilling stress. The AOX pathway maintained the open state of PSII and the stability of the entire photosynthetic electron transport chain. Moreover, the protective role of the AOX pathway on PSII was more important than that on PSI. However, inhibition of the AOX pathway could be compensated by increasing CEF-PSI activity under chilling stress.

Keywords: chlorophyll fluorescence; JIP-test; OJIP curve; salicylhydroxamic acid; *Solanum lycopersicum*.

Introduction

Photosynthesis absorbs light energy and through a photochemical reaction generates reducing equivalents (NADPH), which are provided to carbon assimilation as reducing power (Yoshida *et al*. 2007, Allakhverdiev 2011). However, carbon assimilation is inhibited in plants under abiotic stresses; it reduces the utilization of reducing power and leads to the accumulation of NADPH in the chloroplast stroma (Ort and Baker 2002, Hu *et al*. 2018). Accumulation of reducing equivalents in stroma causes overreduction of the photosynthetic electron transport chain and leads to photoinhibition (Yoshida *et al*. 2007). Excess reducing equivalents generated in chloroplasts can be transferred to mitochondria *via* the malate–oxaloacetate shuttle (Nunes-Nesi *et al*. 2008, Cheng *et al*. 2020).

Highlights

- Chilling inhibited the function of PSII and blocked photosynthetic electron transport in tomato seedlings
- The AOX pathway was more important for PSII than PSI
- The AOX pathway maintained the stability of the electron transport chain during chilling

Received 10 December 2021
Accepted 17 March 2022
Published online 31 March 2022

+Corresponding author
e-mail: huwenhai@jgsu.edu.cn

Abbreviations: CEF-PSI – cyclic electron transport around PSI; ETR – electron transport rate; F_0 – minimal fluorescence yield of the dark-adapted state; F_m – maximal fluorescence yield of the dark-adapted state; F_v/F_m – maximal quantum yield of PSII photochemistry; NPQ – nonphotochemical quenching; OEC – oxygen-evolving complex; OJIP curve – Chl *a* fluorescence transient; PI_{ABS} – performance index for energy conservation from photons absorbed by PSII until the reduction of intersystem electron acceptors; P_m – maximum P_{700} changes; q_P – photochemical quenching coefficient; RC – PSII reaction centre; RC/CS – density of Q_A-reducing PSII reaction centres per cross-section; SHAM – salicylhydroxamic acid; V_{KCN} – AOX pathway capacity; V_T – total respiratory rate; W_K – the normalized relative variable fluorescence at the K step; $Y_{(II)}$ – effective PSII quantum yield; $Y_{(NO)}$ – quantum yield of nonregulated energy dissipation; $Y_{(NPQ)}$ – quantum yield of regulated energy dissipation; Φ_{PSII} – effective quantum yield of PSII photochemistry; φ_{Eo} – quantum yield for electron transport (ET); φ_{Ro} – quantum yield of reduction of end electron acceptors at the PSI acceptor side.

Acknowledgements: This work was supported by the Key Project of Jiangxi Natural Science Foundation (grant no. 20192ACB20017).
Conflict of interest: The authors declare that they have no conflict of interest.

Therefore, the extra-chloroplastic sink for excess reducing equivalents generated by photosynthesis might affect the redox state of the photosynthetic electron transport chain and play a particular role in protecting the photosynthetic apparatus from photoinhibition (Cheng *et al*. 2020).

As the two major energy metabolism centres in green cells, the functions of chloroplasts and mitochondria are closely coordinated (Noguchi and Yoshida 2008). Mitochondrial respiration is considered to be beneficial for optimizing photosynthesis and protecting chloroplasts against photoinhibition (Raghavendra and Padmasree 2003, Alber and Vanlerberghe 2021). Compared to the cytochrome oxidase pathway, the alternative oxidase (AOX) pathway transfers electrons from the ubiquinone pool to oxygen without proton translocation across the inner membrane (Vanlerberghe *et al*. 2009). The AOX pathway provides an extra-chloroplastic means to optimize the status of chloroplast energy pools (ATP and NADPH) under conditions that challenge energy balance in the photosynthetic cell (Vanlerberghe *et al*. 2020). Evidence suggests that the AOX pathway can protect chloroplasts against photoinhibition by dissipating the excess reducing equivalents from chloroplasts under abiotic stressful conditions (Raghavendra and Padmasree 2003, Cheng *et al*. 2020, Garmash 2021). In fact, abiotic stresses, such as chilling (Hu *et al*. 2017), drought (Bartoli *et al*. 2005, Hu *et al*. 2018), salinity (Analin *et al*. 2020, Challabathula *et al*. 2022), and high light (Zhang *et al*. 2012), can increase AOX gene expression and AOX pathway capacity (Clifton *et al*. 2005). Downregulation of the AOX pathway aggravates photoinhibition in illuminated leaves under environmental stresses (Bartoli *et al*. 2005, Yoshida *et al*. 2007, Florez-Sarasa *et al*. 2011, Hu *et al*. 2018). Activation of the AOX pathway can dissipate excessive chloroplastic reducing equivalents and balancec photosynthetic electron transport (Jiang *et al*. 2019, Challabathula *et al*. 2022). Several studies have demonstrated that the photosynthetic rate and PSII photochemical efficiency obviously decrease and that the photosynthetic electron transport chain was more overreduced in AOX-deficient mutants and salicylhydroxamic acid (SHAM, AOX inhibitor)-treated leaves under abiotic stresses (Giraud *et al*. 2008, Yoshida *et al*. 2011, Dahal and Vanlerberghe 2018, Zheng *et al*. 2021, Challabathula *et al*. 2022). AOX overexpression in tobacco was shown to improve photosynthetic performance compared with the wild type under drought conditions (Dahal *et al*. 2015). Gandin *et al*. (2012) observed that a lack of AOX decreased the activities of NADP-malate dehydrogenase and NAD-malate dehydrogenase, two key enzymes in the malate–oxaloacetate shuttle, and increased the NADPH/$NADP^+$ ratio within the stroma in the *Arabidopsis thaliana aox1a* mutant compared to the wild type. Cheng *et al*. (2020) also reported that malate–oxaloacetate shuttle activity and AOX pathway activity were synchronously enhanced with increasing light intensity both in control and chill-treated *Rumex* K-1 leaves and that inhibition of the AOX pathway led to more severe accumulation of hydrogen peroxide and photoinhibition in chill-treated leaves.

Chilling is a major factor limiting the productivity and geographical distribution of many tropical and subtropical crops (Allen and Ort 2001). Chilling inhibits photosynthesis *via* stomatal closure and loss of activity of Calvin cycle enzymes, such as isoheptanone-1,7-diphosphatase, fructose-1,6-diphosphatase, and Rubisco (Gan *et al*. 2019, Ramazan *et al*. 2021), which leads to overreduction of the photosynthetic electron transport chain. Chilling also increases AOX synthesis and the capacity of the AOX pathway (Kiener and Bramlage 1981, Grabelnych *et al*. 2014, Ikkonen *et al*. 2020). In our previous study, chilling induced upregulation of the AOX pathway in cucumber leaves, which played a critical role in protection against chill-induced photoinhibition by avoiding overreduction of photosynthetic electron transport (Hu *et al*. 2017). Cheng *et al*. (2020) also observed that the AOX pathway was upregulated and acted as an extra-chloroplastic sink for excess reducing equivalents generated by photosynthesis in *Rumex* K-1 leaves experiencing chilling stress. According to microarray analyses in AOX antisense-treated *Arabidopsis thaliana*, transcripts for eight genes associated with photosynthetic light reactions were shown to be affected by AOX; however, no transcripts associated with dark reactions changed (Umbach *et al*. 2005). These results indicate that the AOX pathway has a direct influence on the photosynthetic electron transport chain; however, few studies have attempted to explore the role of the AOX pathway in the protection of components of the photosynthetic electron transport chain in chilled plants. In the present work, we examined the effects of the inhibition of the AOX pathway by SHAM on chlorophyll (Chl) fluorescence and Chl *a* fluorescence transients in tomato seedlings under chilling conditions. The aim of this study was to evaluate the impact of the AOX pathway on energy metabolism in chloroplasts and explore the protective role of the AOX pathway on the photosynthetic apparatus of chill-exposed tomato seedlings.

Materials and methods

Plant materials, growth conditions, and experimental design: Experiments were conducted at the Jingganshan University, Jiangxi Province, China. Tomato (*Solanum lycopersicum* cv. Alisa Craig) seeds were sown in a plastic tray (5-cm depth, 20-cm length, and 14-cm width) thoroughly filled with peat (*Sphagnum* moss, 5–20 mm, *Pindstrup*, Denmark) in an artificial climate chamber. Seedlings at the two-leaf stage were transferred into a plastic pot (15-cm depth and 15-cm diameter) filled with peat and watered daily with a half-strength Enshi nutrient solution (Yu and Matsui 1997). The artificial climate chamber environmental conditions were as follows: a 12-h photoperiod, temperatures of 28/18°C (day/night), and PPFD of 500 μmol m^{-2} s^{-1}.

SHAM and chilling treatment started when plants were in the six-leaf stage. On the day before chilling treatment, plants were divided into two groups. One group was still cultured in the artificial chamber. The other group was transferred into a climate box (*ZRY-YY1000*, *SAFU Experimental Apparatus Technology*, Ningbo, China)

with a 12-h photoperiod, PPFD of 200 μmol m^{-2} s^{-1}, and a temperature of 8°C for the chilling treatment. Both groups of plants were sprayed with 1 mM SHAM solutions or distilled water (containing the same concentration of ethanol as the controls) before and 2 d after chilling treatments. SHAM was dissolved in a minimal volume of ethanol and then brought up to volume with distilled water. The four treatments employed were as follows: (*1*) normal temperature treatment (NT): plants were cultured in an artificial climate chamber at 28/18°C (day/night) and sprayed with distilled water; (*2*) normal temperature with SHAM treatment (NT + SHAM): plants were cultured in an artificial climate chamber at 28/18°C (day/night) and sprayed with 1 mM SHAM; (3) chilling treatment (CL): plants were cultured in an artificial climate box at 8°C and sprayed with distilled water; and (*4*) chilling with SHAM treatment (CL + SHAM): plants were cultured in an artificial climate box at 8°C and sprayed with 1 mM SHAM. There were five replications per treatment. The respiratory rate, Chl fluorescence, and Chl *a* fluorescence transients in the first fully expanded leaf were measured 4 d after treatment.

Respiratory rate measurement: The respiratory rate was measured using a Clark-type oxygen electrode (*Oxygraph*, *Hansatech Instruments*, Norfolk, UK) at 25°C according to methods outlined in Cheng *et al.* (2020). Before the respiratory measurements, the samples (0.1 g of fresh mass) were kept in the dark for 10 min. Total respiration (V_T) was defined as the O_2 uptake rate without any inhibitor, and the AOX pathway capacity (V_{KCN}) was defined as the O_2 uptake rate in the presence of KCN (10 mM) in this study.

Simultaneous measurements of Chl fluorescence and P_{700}: Chl fluorescence and P_{700} were synchronously measured with the *Fluo + P700 Measuring Mode* of the *Dual-PAM-100/F* (*Walz*, Effeltrich, Germany) according to the instruction manual for *DUAL-PAM-100*. After the dark adaptation for 30 min, the minimal fluorescence yield (F_0) and maximal fluorescence yield (F_m) of the dark-adapted state were measured. An actinic light [500 μmol(photon) m^{-2} s^{-1}] was then applied for 240 s to obtain light-adapted Chl fluorescence and P_{700} parameters. The determined parameters included the maximal P_{700} changes (P_m), maximal quantum yield of PSII photochemistry (F_v/F_m), effective PSII quantum yield [$Y_{(II)}$], quantum yield of regulated energy dissipation [$Y_{(NPQ)}$], quantum yield of nonregulated energy dissipation [$Y_{(NO)}$], photochemical quenching coefficient (q_P), non-photochemical quenching (NPQ), and electron transport rate (ETR). The cyclic electron transport around PSI (CEF-PSI) was estimated by $ETR_{(I)}/ETR_{(II)}$ (Yamori *et al.* 2011).

Chl *a* fluorescence transient and JIP-test: The Chl *a* fluorescence transient (OJIP curve) was measured by a plant efficiency analyser (*Handy PEA*, *Hansatech Instruments Ltd*., Norfolk, UK). Leaves were dark-adapted for 30 min using special leaf clips. The OJIP curve was induced by red actinic light [wavelength at peak 650 nm, 2,000 μmol(photon) m^{-2} s^{-1}], and 2 s of transient fluorescence was recorded. Based on the model in 'Theory of Energy Fluxes in Biomembranes', the OJIP curves were analysed using the JIP-test. This analysis took into consideration several pieces of basic fluorescence data at 20 μs (F_0, step O), 300 μs (F_K, step K), 2 ms (F_J, step J), 30 ms (F_I, step I), and maximum yield (F_m, which is equal to F_P, step P). Then, JIP-test parameters were examined in the experiment according to methods outlined in Chen *et al.* (2014): (*1*) The normalized relative variable fluorescence at the K step, $W_K = (F_K - F_0)/(F_J - F_0)$; (*2*) performance index for energy conservation from photons absorbed by PSII until the reduction of intersystem electron acceptors, $PI_{ABS} = (RC/ABS) \times [\varphi_{Po}/(1 - \varphi_{Po})] \times [\psi_0/(1 - \psi_0)]$; (*3*) density of Q_A-reducing PSII reaction centres (RC) per cross-section (CS), $RC/CS = \varphi_{Po} \times (V_J/M_0) \times (ABS/CS)$; (*4*) quantum yield of electron transport, $\varphi_{Eo} = [1 - (F_0/F_m)] \times (1 - V_J)$; and (*5*) quantum yield of reduction of end electron acceptors at the PSI acceptor side, $\varphi_{Ro} = [1 - (F_0/F_m)] \times (1 - V_I)$.

Statistical analysis: The results are reported as the means with standard errors (SEs). The significance of the results was checked by the least-significant difference (LSD) test at $p<0.05$ using *PASW Statistics 18* (*SPSS Inc.*, Chicago, IL, USA) *via* one-way analysis of variance (*ANOVA*).

Results

Respiration: Compared to normal temperature conditions, the total respiratory rate decreased, but the AOX pathway capacities increased by 66.7% in chilling-treated tomato seedlings (Fig. 1). To determine the function of AOX in the protection of the photosynthetic apparatus in tomato seedlings under chilling stress, AOX activity was inhibited by feeding 1 mM SHAM to intact leaves. *In vivo* AOX pathway capacities were reduced by approximately 50.0 and 52.5% in SHAM-treated seedlings under normal temperature and chilling conditions, respectively (Fig. 1).

Chl fluorescence parameters: SHAM treatment had no effect on the F_v/F_m and P_m in tomato seedlings under normal temperature conditions (Fig. 2), showing that 1 mM SHAM did not inhibit PSII and PSI activity in this experiment. Chilling induced a decrease in F_v/F_m, which was aggravated by SHAM treatment. SHAM treatment caused a decrease in F_v/F_m of 22.5% in tomato seedlings subjected to chilling stress. Although there was no significant difference, chilling also induced a decrease in P_m by 18.9%. However, SHAM treatment did not affect P_m in tomato seedlings under normal temperature or chilling conditions (Fig. 2).

The complementary PSII quantum yields [$Y_{(II)} + Y_{(NPQ)} + Y_{(NO)} = 1$] were significantly affected by chilling stress (Table 1). Chilling induced a decrease in $Y_{(II)}$ by 39.3%, while $Y_{(NPQ)}$ and $Y_{(NO)}$ increased by 85.2 and 19.8%, respectively. SHAM treatment aggravated the decrease in $Y_{(II)}$ and the increase in $Y_{(NO)}$ induced by chilling. However,

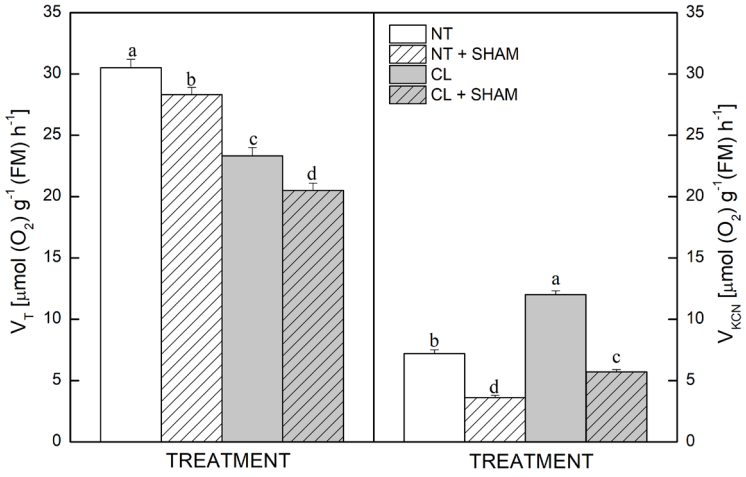

Fig. 1. Effects of salicylhydroxamic acid (SHAM, 1 mM) and chilling (8°C) on total respiratory rate (V_T) and AOX pathway capacity (V_{KCN}) in tomato seedlings after 4 d of treatment. NT – normal temperature treatment; NT + SHAM – normal temperature with SHAM treatment; CL – chilling treatment; CL + SHAM – chilling with SHAM treatment. Data are the means of independent measurements of five replicates with standard errors. Values followed by *different letters* are significantly different at the 0.05% level.

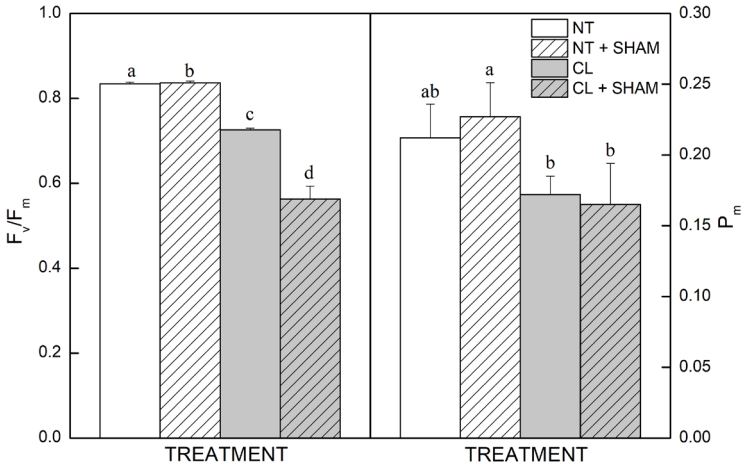

Fig. 2. Effects of salicylhydroxamic acid (SHAM, 1 mM) and chilling (8°C) on maximal quantum yield of PSII photochemistry (F_v/F_m) and maximum P_{700} changes (P_m) in tomato seedlings after 4 d of treatment. NT – normal temperature treatment; NT + SHAM – normal temperature with SHAM treatment; CL – chilling treatment; CL + SHAM – chilling with SHAM treatment. Data are the means of independent measurements of five replicates with standard errors. Values followed by *different letters* are significantly different at the 0.05% level.

$Y_{(NPQ)}$ significantly decreased in tomato seedlings under chilling conditions with SHAM treatment. Under normal temperature, SHAM treatment decreased $Y_{(II)}$ by 17.2% but increased $Y_{(NPQ)}$ by 52.6%, which did not affect $Y_{(NO)}$.

The q_P, $ETR_{(II)}$, and $ETR_{(I)}$ of tomato seedlings decreased under chilling stress (Table 1). Compared to NT, the chilling treatment significantly decreased the q_P, $ETR_{(II)}$, and $ETR_{(I)}$ values by 18.0, 39.3, and 28.3%, respectively. Moreover, SHAM treatment caused further decreases in the q_P, $ETR_{(II)}$, and $ETR_{(I)}$ of chilled tomato seedlings of 10.0, 13.5, and 9.7%, respectively. Under normal temperature conditions, SHAM treatment also decreased q_P, $ETR_{(II)}$, and $ETR_{(I)}$ by 12.3, 17.2, and 9.1%, respectively.

Chilling significantly induced increases in NPQ and $ETR_{(I)}/ETR_{(II)}$, which increased by 53.2 and 17.9%, respectively, compared to NT treatment (Table 1). There was no obvious change in $ETR_{(I)}/ETR_{(II)}$ under chilling conditions with/without SHAM treatment. However, NPQ significantly decreased by chilling with SHAM treatment (CL + SHAM), which was significantly lower than the value of NT and CL treatment. Under normal temperature conditions, SHAM treatment induced an increase in NPQ by 56.9% but had no effect on $ETR_{(I)}/ETR_{(II)}$.

OJIP curves and JIP-test parameters: Under normal temperature conditions, SHAM treatment only decreased the P step. However, OJIP curves from chilling-treated seedlings showed a sharp depression at the J, I, and P steps, which were aggravated by SHAM treatment (Fig. 3). It was observed that there were no differences in W_K between the four treatments in this experiment (Table 2). Chilling decreased RC/CS, PI_{ABS}, and φ_{Eo} by 54.5, 86.4, and 44.3%, respectively, which were significantly aggravated by SHAM treatment. CL + SHAM treatment significantly decreased RC/CS, PI_{ABS}, and φ_{Eo} by 48.5, 79.9, and 51.4%, respectively, compared to tomato seedlings subjected to chilling stress. Under normal temperature conditions, SHAM treatment also decreased RC/CS, PI_{ABS}, and φ_{Eo} by 10.3, 34.0, and 10.7%, respectively. Chilling also decreased φ_{Ro} by 8.7%, even though it was not statistically significant. However, SHAM treatment significantly decreased φ_{Ro} by 58.9% under chilling treatment (Table 2).

Discussion

Salicylhydroxamic acid (SHAM), a well-known inhibitor of the mitochondrial AOX pathway, has been extensively

Table 1. Effects of salicylhydroxamic acid (SHAM, 1 mM) and chilling (8°C) on chlorophyll fluorescence parameters in tomato seedlings after 4 d of treatment. NT – normal temperature treatment; NT + SHAM – normal temperature with SHAM treatment; CL – chilling treatment; CL + SHAM – chilling with SHAM treatment. Data are the means of independent measurements of five replicates with standard errors. Values followed by *different letters* are significantly different at the 0.05% level. ETR – electron transport rate; NPQ – nonphotochemical quenching; q_P – photochemical quenching coefficient; $Y_{(II)}$ – effective PSII quantum yield; $Y_{(NPQ)}$ – quantum yield of regulated energy dissipation; $Y_{(NO)}$ – quantum yield of nonregulated energy dissipation.

Parameter	NT	NT + SHAM	CL	CL + SHAM
$Y_{(II)}$	0.552 ± 0.013^{a}	0.457 ± 0.017^{b}	0.335 ± 0.006^{c}	0.261 ± 0.013^{d}
$Y_{(NPQ)}$	0.196 ± 0.013^{c}	0.299 ± 0.006^{b}	0.363 ± 0.002^{a}	0.193 ± 0.053^{c}
$Y_{(NO)}$	0.252 ± 0.012^{c}	0.244 ± 0.011^{c}	0.302 ± 0.004^{b}	0.546 ± 0.063^{a}
q_P	0.749 ± 0.019^{a}	0.657 ± 0.028^{b}	0.614 ± 0.013^{b}	0.539 ± 0.021^{c}
NPQ	0.784 ± 0.070^{b}	1.230 ± 0.027^{a}	1.201 ± 0.014^{a}	0.388 ± 0.147^{c}
$ETR_{(II)}$	116 ± 3^{a}	96 ± 4^{b}	70 ± 1^{c}	55 ± 3^{d}
$ETR_{(I)}$	146 ± 1^{a}	133 ± 6^{b}	105 ± 3^{c}	91 ± 5^{d}
$ETR_{(I)}/ETR_{(II)}$	1.262 ± 0.033^{c}	1.383 ± 0.009^{cb}	1.488 ± 0.054^{ab}	1.657 ± 0.103^{a}

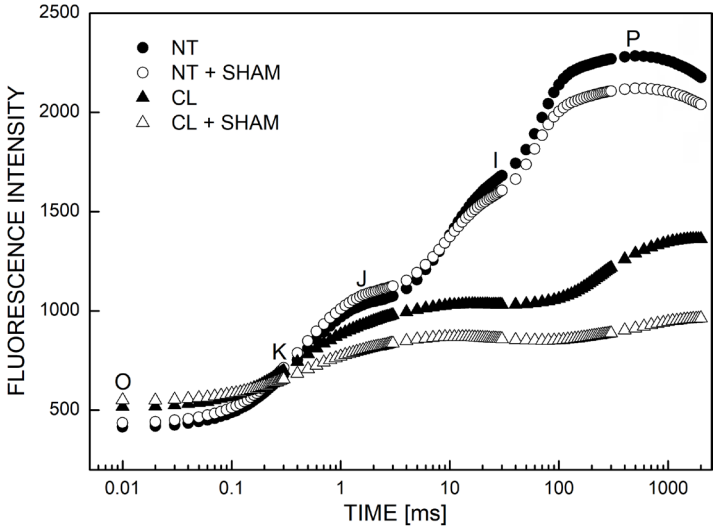

Fig. 3. Effects of salicylhydroxamic acid (SHAM, 1 mM) and chilling (8°C) on Chl *a* fluorescence transient (OJIP curve) in tomato seedlings after 4 d of treatment. NT – normal temperature treatment; NT + SHAM – normal temperature with SHAM treatment; CL – chilling treatment; CL + SHAM – chilling with SHAM treatment. Each curve is the average of five replicates.

Table 2. Effects of salicylhydroxamic acid (SHAM, 1 mM) and chilling (8°C) on JIP-test parameters in tomato seedlings after 4 d of treatment. NT – normal temperature treatment; NT + SHAM – normal temperature with SHAM treatment; CL – chilling treatment; CL + SHAM – chilling with SHAM treatment. Data are the means of independent measurements of five replicates with standard errors. Values followed by *different letters* are significantly different at the 0.05% level. PI_{ABS} – performance index for energy conservation from photons absorbed by PSII until the reduction of intersystem electron acceptors; RC/CS – density of Q_A-reducing PSII reaction centres per cross-section; W_K – the normalized relative variable fluorescence at the K step; φ_{Eo} – quantum yield for electron transport (ET); φ_{Ro} – quantum yield of reduction of end electron acceptors at the PSI acceptor side.

Parameter	NT	NT + SHAM	CL	CL + SHAM
W_K	0.437 ± 0.019^{a}	0.439 ± 0.019^{a}	0.436 ± 0.018^{a}	0.415 ± 0.017^{a}
PI_{ABS}	5.19 ± 0.21^{a}	3.42 ± 0.15^{b}	0.708 ± 0.13^{c}	0.142 ± 0.05^{d}
RC/CS	$1{,}304 \pm 48^{a}$	$1{,}169 \pm 48^{b}$	593 ± 26^{c}	305 ± 47^{d}
φ_{Eo}	0.541 ± 0.005^{a}	0.483 ± 0.008^{b}	0.301 ± 0.022^{c}	0.146 ± 0.023^{d}
φ_{Ro}	0.264 ± 0.010^{a}	0.241 ± 0.011^{a}	0.241 ± 0.032^{a}	0.099 ± 0.036^{b}

used to address the interaction between chloroplasts and mitochondria (Cheng *et al*. 2020). SHAM (1 mM) was used in this study because the concentration is considered sufficiently low to avoid any possible side effects on the photosynthetic machinery (Bartoli *et al*. 2005, Cheng and Zhang 2021). Half of the activity of the AOX pathway was inhibited when tomato seedlings were treated by 1 mM SHAM under normal temperature or chilling conditions

(Fig. 1), which was consistent with our previous study in cucumber (Hu *et al*. 2017). Bartoli *et al*. (2005) also observed that 1 mM SHAM inhibits AOX pathway activity by approximately 70% in leaves from both well-irrigated and water-stressed plants. In our study, 1 mM SHAM did not affect F_v/F_m, P_m, or $Y_{(NO)}$ but decreased $Y_{(II)}$, q_P, $ETR_{(II)}$, and $ETR_{(I)}$ in tomato seedlings under normal temperature conditions [18/28°C (day/night) with 500 µmol(photon) m^{-2} s^{-1}] (Table 1, Fig. 2). These results seemed to indicate that 1 mM SHAM affects the photosynthetic machinery. However, we believe that these results further prove the role of the AOX pathway as an electron sink to protect the photosynthetic apparatus against photoinhibition under high light. There were no obvious changes in F_v/F_m and Φ_{PSII} [actual photochemical efficiency of PSII, same as $Y_{(II)}$ in this study] in cucumber leaves treated with 0–1 mM SHAM at 25°C with 200–300 µmol(photon) m^{-2} s^{-1} (Hu *et al*. 2017). Cheng and Zhang (2021) reported little significant difference in Φ_{PSII}, q_P, or NPQ in isolated *Rumex* K-1 chloroplasts in the presence of 0, 0.2, 0.6, or 1 mM SHAM during photosynthetic induction [1,000 µmol(photon) m^{-2} s^{-1}]; however, the decreases in ETR and q_P were followed by an increase in the SHAM concentration in leaves. Therefore, we speculate that 1 mM SHAM does not affect leaf photosynthesis under normal temperature with weak light but may influence the photosynthetic machinery of leaves under normal temperature with high light. Compared to wild-type plants, *aox1a* plants (AOX1a knockout mutants of *Arabidopsis thaliana*) did not show any changes in photosynthetic parameters under low light [50 µmol(photon) m^{-2} s^{-1}], but photosynthetic parameters related to PSII decreased in *aox1a* plants upon exposure to high light [700 µmol(photon) m^{-2} s^{-1}] conditions (Vishwakarma *et al*. 2014). We also observed that SHAM treatment increased $Y_{(NPQ)}$ and NPQ but did not affect $ETR_{(I)}/ETR_{(II)}$, which suggested that the decrease in the AOX pathway could be compensated for by the increase in thermal energy dissipation (Table 1).

As the mitochondrial energy-dissipating system, the AOX pathway is believed to play an important role in protecting chloroplasts against photoinhibition by dissipating excess reducing equivalents from chloroplasts (Raghavendra and Padmasree 2003, Cheng *et al*. 2020). Watanabe *et al*. (2016) reported that a lack of AOX results in overreduction of the photosynthetic electron transport chain and that *Arabidopsis aox1a* mutants under high light conditions are more sensitive to photoinhibition. Some reports show that the AOX pathway is upregulated in winter wheat (Grabelnych *et al*. 2014), cucumber (Hu *et al*. 2017), and *Rumex* K-1 leaves (Cheng *et al*. 2020) subjected to chilling. We observed that AOX pathway capacity increased by 66.7% in tomato seedlings exposed to 8°C for 4 d (Fig. 1), while the chill-induced decreases in F_v/F_m, $ETR_{(II)}$, and $ETR_{(I)}$ were aggravated by inhibition of the AOX pathway (Table 1), which indicated that upregulation of the AOX pathway could protect against chill-induced photoinhibition by optimizing photosynthetic electron transport. Further analysis showed that chilling treatment decreased the values of $ETR_{(II)}$ and $ETR_{(I)}$ by 39.3 and 28.3%, respectively, and that SHAM treatment caused a further decrease in $ETR_{(II)}$ and $ETR_{(I)}$ by 13.5 and 9.7%, respectively (Table 1). These results indicated that the response of electron transport in PSII was more sensitive than electron transport in PSI to chilling stress and that the AOX pathway played an important role in maintaining electron transport, especially in PSII.

Chilling-sensitive plants exhibit marked physiological dysfunction when exposed to nonfreezing temperatures below approximately 10 to 12°C (Lyons 1973). As the primary targets for chilling stress, the susceptibility of PSII and PSI to chilling depends on plant species and stressful conditions (Sonoike 1996, Bertamini *et al*. 2005, Li and Zhang 2016). Sonoike (1996) commented that the relative quantum yield of PSII is decreased at chilling temperatures and that the dependence on temperature is almost linear, without a specific threshold temperature; however, weak illumination [approximately 100 µmol(photon) m^{-2} s^{-1}] is essential for the selective photoinhibition of PSI in chilling-sensitive plants at chilling temperatures. Huang *et al*. (2010) also reported that PSII is more sensitive to chilling temperatures under moderate light than PSI in tropical trees and that the photoinhibition of PSII and closure of PSII reaction centres can serve to protect PSI. In this study, the relative fluorescence intensity at point P of the OJIP curve decreased significantly (Fig. 3), and F_v/F_m and PI_{ABS} declined by 13.0 and 86.4% (Table 2), respectively, in chilled tomato seedlings, which indicated that chilling led to a decrease in the photochemical activity of PSII. P_m can be used to estimate PSI activity (Takagi *et al*. 2017). Chilling decreased P_m by 18.9%, but there was no statistically significant difference ($p<0.05$) between the normal temperature and the chilling treatments (Fig. 2). This result suggested that chilling also affected PSI, but the heterogeneity of PSI was greater than that of PSII in chilled tomato seedlings. However, we observed that SHAM treatment exacerbated the decline in F_v/F_m and PI_{ABS} but had no effect on P_m (Tables 1, 2; Fig. 2), indicating that the protective role of the AOX pathway on PSII was more important than that of PSI.

The photons absorbed by PSII are converted into chemically fixed energy by photochemical charge separation at PSII reaction centres (Kramer *et al*. 2004). $Y_{(II)}$ is an estimate of the fraction of photons utilized by PSII photochemistry, and q_P is an estimate of the proportion of oxidized PSII centres (Maxwell and Johnson 2000). In this study, chilling decreased $Y_{(II)}$ and q_P by 39.3 and 18.0%, respectively (Table 1), which suggested that chilling decreased the utilization of absorbed light energy in chloroplasts by the closure of PSII. The decrease in RC/CS under chilling stress (Table 2) further indicated that chilling led to the inactivation of PSII reaction centres and decreased the density of active PSII reaction centres (Zhang *et al*. 2020). We observed that the inhibition of AOX pathway activity caused significant decreases in $Y_{(II)}$, q_P, and RC/CS in tomato seedlings under both normal temperature and chilling conditions (Tables 1, 2). These results indicated that the AOX pathway is important to maintain the open state of PSII, which could contribute to protection against chill-induced photoinhibition.

OJIP transients reflect the structural stability of PSII, as they provide complete insight into energy fluxes between different components of PSII (Akhter *et al*. 2021). Chilling changed the shape of the OJIP curves, especially decreasing the I and P steps (Fig. 3), indicating a disturbance in structural stability at various points of PSII. SHAM treatment aggravated the depression at the J, I, and P steps, which suggested that the AOX pathway played an important role in the structural stability of PSII under chilling stress. However, the K peak in the OJIP curves and W_K did not change under chilling conditions with/without SHAM treatment (Fig. 3, Table 2), which indicated that the OEC on the donor side of PSII was not affected by chilling and the AOX pathway. Damage to OEC is always associated with the appearance of a K peak in the OJIP curves and an increase in W_K (Strasser *et al*. 1995, Dąbrowski *et al*. 2019). φ_{Eo} refers to the quantum yield of PSII electron transport (Chen *et al*. 2014), and φ_{Ro} reflects the quantum yield for the reduction of the end electron acceptors at the PSI acceptor side (Guo *et al*. 2020). In this study, chilling significantly decreased φ_{Eo} by 51.4% but resulted in a nonsignificant decrease of 8.7% in φ_{Ro} (Table 2). These results reflected that the chill-induced inhibition of electron transfer on the PSII acceptor side was more serious than that on the PSI acceptor side. Compared to chilling stress, SHAM treatment aggravated the decrease in φ_{Eo} and φ_{Ro} by 51.4 and 59.0%, respectively, indicating that the AOX pathway played an important role in maintaining the stability of the entire photosynthetic electron transport chain.

Thermal energy dissipation and CEF-PSI are the major photoprotective mechanisms to protect the photosynthetic apparatus in chloroplasts (Lei *et al*. 2014). The $ETR_{(I)}/ETR_{(II)}$ ratio is an estimate of CEF-PSI activation, and $ETR_{(I)}$ is larger than $ETR_{(II)}$ if CEF-PSI is functioning (Yamori *et al*. 2011). In the present study, chilling induced increases in NPQ and $ETR_{(I)}/ETR_{(II)}$ of 53.2 and 17.9%, respectively (Table 1). These results showed that chilling induced the enhancement of thermal energy dissipation and CEF-PSI in tomato seedlings and that thermal energy dissipation played a major role in the photoprotection of chill-induced photoinhibition. We also observed that $Y_{(NPQ)}$ strongly increased in tomato seedlings under chilling stress (Table 1). A high $Y_{(NPQ)}$ indicates that plants have retained the physiological means to protect themselves by regulating energy dissipation, such as the dissipation of excessive excitation energy into harmless heat. However, a decrease in NPQ was observed in tomato seedlings under chilling conditions with SHAM treatment. We speculated that the decreases were due to photodamage of the photosynthetic apparatus by excessive excitation energy in PSII. In a previous study, we also observed the same phenomenon in cucumber treated by chilling with high light (Hu *et al*. 2017). Furthermore, we observed that inhibition of the AOX pathway induced a nonsignificant decrease of 11.4% in $ETR_{(I)}/ETR_{(II)}$ of tomato seedlings under chilling stress, implying that the decrease in AOX pathway activity could be compensated by an increase in CEF-PSI. It is well known that CEF-PSI is essential for protecting PSII against excess excitation pressure and that the stability of PSI is essential for the stimulation of CEF-PSI (Lei *et al*. 2014).

In conclusion, chilling stress inhibited photosynthetic electron transport and the response of electron transport in PSII was more sensitive than that in PSI. Chilling stress led to the inactivation of PSII reaction centres and blocked electron transport at the PSII acceptor side but did not affect OEC on the donor side of PSII. Chilling induced the enhancement of thermal energy dissipation and CEF-PSI, and thermal energy dissipation played a major role in photoprotection of chill-induced photoinhibition. Chilling induced upregulation of the AOX pathway, which plays an important role in protection against chill-induced photoinhibition. The protective role was due to improving the function of PSII and the stability of the entire photosynthetic electron transport chain. Moreover, the protective role of the AOX pathway on PSII was more important than that on PSI. However, inhibition of the AOX pathway could be compensated for by increasing CEF-PSI activity under chilling stress.

References

Akhter M.S., Noreen S., Mahmood S. *et al*.: Influence of salinity stress on PSII in barley (*Hordeum vulgare* L.) genotypes, probed by chlorophyll-*a* fluorescence. – J. King Saud Univ. Sci. **33**: 101239, 2021.

Alber N.A., Vanlerberghe G.C.: The flexibility of metabolic interactions between chloroplasts and mitochondria in *Nicotiana tabacum* leaf. – Plant J. **106**: 1625-1646, 2021.

Allakhverdiev S.I.: Recent progress in the studies of structure and function of photosystem II. – J. Photoch. Photobio. B **104**: 1-8, 2011.

Allen D.J., Ort D.R.: Impacts of chilling temperatures on photosynthesis in warm-climate plants. – Trends Plant Sci. **6**: 36-42, 2001.

Analin B., Mohanan A., Bakka K., Challabathula D.: Cytochrome oxidase and alternative oxidase pathways of mitochondrial electron transport chain are important for the photosynthetic performance of pea plants under salinity stress conditions. – Plant Physiol. Bioch. **154**: 248-259, 2020.

Bartoli C.G., Gomez F., Gergoff G. *et al*.: Up-regulation of the mitochondrial alternative oxidase pathway enhances photosynthetic electron transport under drought conditions. – J. Exp. Bot. **56**: 1269-1276, 2005.

Bertamini M., Muthuchelian K., Rubinigg M. *et al*.: Photoinhibition of photosynthesis in leaves of grapevine (*Vitis vinifera* L. cv. Riesling). Effect of chilling nights. – Photosynthetica **43**: 551-557, 2005.

Challabathula D., Analin B., Mohanan A., Bakka K.: Differential modulation of photosynthesis, ROS and antioxidant enzyme activities in stress-sensitive and -tolerant rice cultivars during salinity and drought upon restriction of COX and AOX pathway of mitochondrial oxidative electron transport. – J. Plant Physiol. **268**: 153583, 2022.

Chen S., Strasser R.J., Qiang S.: *In vivo* assessment of effect of phytotoxin tenuazonic acid on PSII reaction centers. – Plant Physiol. Bioch. **84**: 10-21, 2014.

Cheng D., Gao H., Zhang L.: Upregulation of mitochondrial alternative oxidase pathway protects photosynthetic apparatus against photodamage under chilling stress in *Rumex* K-1 leaves. – Photosynthetica **58**: 1116-1121, 2020.

Cheng D.D., Zhang L.T.: Mitochondrial alternative oxidase pathway acts as an electron sink during photosynthetic

induction in *Rumex* K-1 leaves. – Photosynthetica **59**: 615-624, 2021.
Clifton R., Lister R., Parker K.L. *et al.*: Stress-induced co-expression of alternative respiratory chain components in *Arabidopsis thaliana*. – Plant Mol. Biol. **58**: 193-212, 2005.
Dąbrowski P., Baczewska-Dąbrowska A.H., Kalaji H.M. *et al.*: Exploration of chlorophyll *a* fluorescence and plant gas exchange parameters as indicators of drought tolerance in perennial ryegrass. – Sensors-Basel **19**: 2736, 2019.
Dahal K., Martyn G.D., Vanlerberghe G.C.: Improved photosynthetic performance during severe drought in *Nicotiana tabacum* overexpressing a nonenergy conserving respiratory electron sink. – New Phytol. **208**: 382-395, 2015.
Dahal K., Vanlerberghe G.C.: Improved chloroplast energy balance during water deficit enhances plant growth: more crop per drop. – J. Exp. Bot. **69**: 1183-1197, 2018.
Florez-Sarasa I., Flexas J., Rasmusson A.G. *et al.*: *In vivo* cytochrome and alternative pathway respiration in leaves of *Arabidopsis thaliana* plants with altered alternative oxidase under different light conditions. – Plant Cell Environ. **34**: 1373-1383, 2011.
Gan P., Liu F., Li R.B. *et al.*: Chloroplasts – beyond energy capture and carbon fixation: tuning of photosynthesis in response to chilling stress. – Int. J. Mol. Sci. **20**: 5046, 2019.
Gandin A., Duffes C., Day D.A., Cousins A.B.: The absence of alternative oxidase AOX1a results in altered response of photosynthetic carbon assimilation to increasing CO_2 in *Arabidopsis thaliana*. – Plant Cell Physiol. **53**: 1627-1637, 2012.
Garmash E.V.: Role of mitochondrial alternative oxidase in the regulation of cellular homeostasis during development of photosynthetic function in greening leaves. – Plant Biol. **23**: 221-228, 2021.
Giraud E., Ho L.H.M., Clifton R. *et al.*: The absence of ALTERNATIVE OXIDASE1a in *Arabidopsis* results in acute sensitivity to combined light and drought stress. – Plant Physiol. **147**: 595-610, 2008.
Grabelnych O.I., Borovik O.A., Tauson E.L. *et al.*: Mitochondrial energy-dissipating systems (alternative oxidase, uncoupling proteins, and external NADH dehydrogenase) are involved in development of frost-resistance of winter wheat seedlings. – Biochemistry-Moscow **79**: 506-519, 2014.
Guo Y., Zhang Y., Liu Y. *et al.*: Effect of AtLFNR1 deficiency on chlorophyll *a* fluorescence rise kinetics OJIP of *Arabidopsis*. – Photosynthetica **58**: 391-398, 2020.
Hu W.H., Yan X.H., He Y., Ye X.L.: Role of alternative oxidase pathway in protection against drought-induced photoinhibition in pepper leaves. – Photosynthetica **56**: 1297-1303, 2018.
Hu W.H., Yan X.H., Yu J.Q.: Importance of the mitochondrial alternative oxidase (AOX) pathway in alleviating photoinhibition in cucumber leaves under chilling injury and subsequent recovery when leaves are subjected to high light intensity. – J. Hortic. Sci. Biotech. **92**: 31-38, 2017.
Huang W., Zhang S.B., Cao K.F.: The different effects of chilling stress under moderate light intensity on photosystem II compared with photosystem I and subsequent recovery in tropical tree species. – Photosynth. Res. **103**: 175-182, 2010.
Ikkonen E.N., Grabelnykh O.I., Sherudilo E.G., Shibaeva T.G.: Salicylhydroxamic acid-resistant and sensitive components of respiration in chilling-sensitive plants subjected to a daily short-term temperature drop. – Russ. J. Plant Physiol. **67**: 60-67, 2020.
Jiang Z.X., Watanabe C.K.A., Miyagi A. *et al.*: Mitochondrial AOX supports redox balance of photosynthetic electron transport, primary metabolite balance, and growth in *Arabidopsis thaliana* under high light. – Int. J. Mol. Sci. **20**: 3067, 2019.
Kiener C.M., Bramlage W.J.: Temperature effects on the activity of the alternative respiratory pathway in chill-sensitive *Cucumis sativus*. – Plant Physiol. **68**: 1474-1478, 1981.
Kramer D.M., Johnson G., Kiirats O., Edwards G.E.: New fluorescence parameters for the determination of Q_A redox state and excitation energy fluxes. – Photosynth. Res. **79**: 209-218, 2004.
Lei Y., Zheng Y., Dai K. *et al.*: Different responses of photosystem I and photosystem II in three tropical oilseed crops exposed to chilling stress and subsequent recovery. – Trees **28**: 923-933, 2014.
Li J.W., Zhang S.B.: Differences in the responses of photosystems I and II in *Cymbidium sinense* and *C. tracyanum* to long-term chilling stress. – Front. Plant Sci. **6**: 1097, 2016.
Lyons J.M.: Chilling injury in plants. – Ann. Rev. Plant Physio. **24**: 445-466, 1973.
Maxwell K., Johnson G.N.: Chlorophyll fluorescence – a practical guide. – J. Exp. Bot. **51**: 659-668, 2000.
Noguchi K., Yoshida K.: Interaction between photosynthesis and respiration in illuminated leaves. – Mitochondrion **8**: 87-99, 2008.
Nunes-Nesi A., Sulpice R., Gibon Y., Fernie A.R.: The enigmatic contribution of mitochondrial function in photosynthesis. – J. Exp. Bot. **59**: 1675-1684, 2008.
Ort D.R., Baker N.R.: A photoprotective role for O_2 as an alternative electron sink in photosynthesis? – Curr. Opin. Plant Biol. **5**: 193-198, 2002.
Raghavendra A.S., Padmasree K.: Beneficial interactions of mitochondrial metabolism with photosynthetic carbon assimilation. – Trends Plant Sci. **8**: 546-553, 2003.
Ramazan S., Bhat H.A., Zargar M.A. *et al.*: Combined gas exchange characteristic, chlorophyll fluorescence and response curves as selection traits for temperature tolerance in maize genotypes. – Photosynth. Res. **150**: 213-225, 2021.
Sonoike K.: Photoinhibition of photosystem I: its physiological significance in the chilling sensitivity of plants. – Plant Cell Physiol. **37**: 239-247, 1996.
Strasser R.J., Srivastava A., Govindjee.: Polyphasic chlorophyll *a* fluorescence transient in plants and cyanobacteria. – Photochem. Photobiol. **61**: 32-42, 1995.
Takagi D., Amako K., Hashiguchi M. *et al.*: Chloroplastic ATP synthase builds up a proton motive force preventing production of reactive oxygen species in photosystem I. – Plant J. **91**: 306-324, 2017.
Umbach A.L., Fiorani F., Siedow J.N.: Characterization of transformed *Arabidopsis* with altered alternative oxidase levels and analysis of effects on reactive oxygen species in tissue. – Plant Physiol. **139**: 1806-1820, 2005.
Vanlerberghe G.C., Cvetkovska M., Wang J.: Is the maintenance of homeostatic mitochondrial signaling during stress a physiological role for alternative oxidase? – Physiol. Plantarum **137**: 392-406, 2009.
Vanlerberghe G.C., Dahal K., Alber N. *et al.*: Photosynthesis, respiration and growth: a carbon and energy balancing act for alternative oxidase. – Mitochondrion **52**: 197-211, 2020.
Vishwakarma A., Bashyam L., Senthilkumaran B. *et al.*: Physiological role of AOX1a in photosynthesis and maintenance of cellular redox homeostasis under high light in *Arabidopsis thaliana*. – Plant Physiol. Bioch. **81**: 44-53, 2014.
Watanabe C.K.A., Yamori W., Takahashi S. *et al.*: Mitochondrial alternative pathway-associated photoprotection of photosystem II is related to the photorespiratory pathway. – Plant Cell Physiol. **57**: 1426-1431, 2016.
Yamori W., Sakata N., Suzuki Y. *et al.*: Cyclic electron flow around photosystem I via chloroplast NAD(P)H dehydrogenase

(NDH) complex performs a significant physiological role during photosynthesis and plant growth at low temperature in rice. – Plant J. **68**: 966-976, 2011.

Yoshida K., Terashima I., Noguchi K.: Up-regulation of mitochondrial alternative oxidase concomitant with chloroplast over-reduction by excess light. – Plant Cell Physiol. **48**: 606-614, 2007.

Yoshida K., Watanabe C.K., Terashima I., Noguchi K.: Physiological impact of mitochondrial alternative oxidase on photosynthesis and growth in *Arabidopsis thaliana*. – Plant Cell Environ. **34**: 1890-1899, 2011.

Yu J.Q., Matsui Y.: Effects of roots exudates and allelochemicals on ion uptake by cucumber seedlings. – J. Chem. Ecol. **23**: 817-827, 1997.

Zhang L.T., Xu R., Liu J.G.: Efficacy of botanical pesticide for rotifer extermination during the cultivation of *Nannochloropsis oculata* probed by chlorophyll *a* fluorescence transient. – Photosynthetica **58**: 156-162, 2020.

Zhang L.T., Zhang Z.S., Gao H.Y. *et al*.: The mitochondrial alternative oxidase pathway protects the photosynthetic apparatus against photodamage in *Rumex* K-1 leaves. – BMC Plant Biol. **12**: 40, 2012.

Zheng J., Fang C., Ru L. *et al*.: Glutathione-ascorbate cycle and photosynthetic electronic transfer in alternative oxidase-manipulated waterlogging tolerance in watermelon seedlings. – Horticulturae **7**: 130, 2021.